NUCLEAR THEORY, Vol. 33 (2014)
eds. A.I. Georgieva, N. Minkov, Heron Press, Sofia

Reaction Mechanisms Involved in the Deuteron Interaction with Nuclei

M. Avrigeanu, **V. Avrigeanu**, **C. Mănăilescu**

Horia Hulubei National Institute for Physics and Nuclear Engineering,
P.O. Box MG-6, 077125 Bucharest-Magurele, Romania

Abstract. An extended analysis of the reaction mechanisms involved in the deuterons interaction with nuclei, namely the breakup, stripping, pick-up, pre-equilibrium (PE) emission, as well as the evaporation from fully equilibrated compound nucleus (CN), is presented. The overall agreement of the measured data and model–calculation results proves the correctness of nuclear mechanism description used for the deuteron–nucleus interaction, while the discrepancies of the newest evaluated data within the TENDL-2013 library stress out the strong effects of the direct processes.

1 Introduction

The improvement of the nuclear databases for the assessment of the induced radioactivity and the radiation damage to structural components of the international large-scale facilities as ITER (International Thermonuclear Experimental Reactor) [1], IFMIF (International Fusion Material Irradiation Facility) [2], and SPIRAL-2 (Systéme de Production d'Ions Radioactifs en Ligne - generation 2) [3], highly requests to update the theoretical frame of the deuteron activation cross sections calculations by a unitary and consistent analysis of the reaction mechanisms involved.

The description of deuteron-nucleus interaction represents an important test for both the appropriateness of reaction mechanism models and the evaluation of nuclear data requested especially by the above mentioned research programmes. The weak binding energy of the deuteron, B=2.224 MeV, is responsible for the high complexity of the interaction process that supplementary involves a variety of reactions initiated by the neutrons and protons following the deuteron breakup. Next, usually neglected or very poorly taken into account, the (d,p) and (d,n) stripping as well as the (d,t) and (d,α) pick-up reactions contributions have been shown to be important at low incident energies, requesting an appropriate treatment within, e.g., the Coupled-Reaction Channels (CRC) formalism. Thus, the present work concerns a deeper understanding of deuteron breakup, stripping and pick-up reactions, all together and consistently with the better-known and described statistical emission [4–7].

2 Deuteron Breakup

The physical picture of the deuteron breakup (BU) in the Coulomb and nuclear fields of the target nucleus considers two distinct processes, namely the elastic breakup (EB) in which the target nucleus remains in its ground state and none of the deuteron constituents interacts with it, and the inelastic breakup or breakup fusion (BF), where one of these deuteron constituents interacts with the target nucleus while the remaining one is detected.

The former parametrization of the total nucleon–emission breakup cross sections was given by Kalbach [8] as a function of the deuteron incident energy E and mass number A of the target nucleus:

$$\sigma_{BU}^{b} = K_{d,b}\frac{(A^{1/3}+0.8)^2}{1+exp(\frac{13-E}{6})}, \;\; K_{d,p}=21, \;\; K_{d,n}=18 \;\; . \qquad (1)$$

The corresponding total proton–emission breakup cross sections for deuteron interactions with target nuclei from ^{56}Fe to ^{231}Pa are shown in Figure 1.

Additional features of the breakup cross–section parametrization in terms of the deuteron total–reaction cross section σ_R have been considered by Avrigeanu *et al.* [4], namely the dependence on the target charge number Z, while distinct forms are provided for the total BU nucleon emission as well as the EB and BF

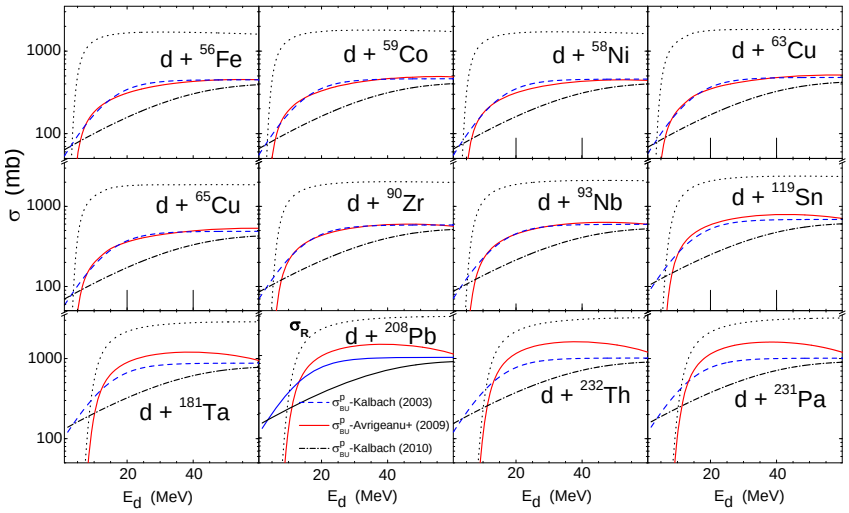

Figure 1. The energy dependence of the total proton–emission breakup cross sections given by the parametrizations of Refs. [4] (solid curves), [8] (dashed curves), and [9] (dash–dotted curves), for deuteron interactions with target nuclei from ^{56}Fe to ^{231}Pa. The deuteron total reaction cross sections [11] are shown by dotted curves.

components:

$$\sigma_{BU}^{p/n} = [0.087 - 0.0066Z + 0.00163ZA^{1/3} + 0.0017A^{1/3}E - 0.000002ZE^2]\sigma_R \ , \quad (2)$$

$$\sigma_{EB} = [0.031 - 0.0028Z + 0.00051ZA^{1/3} + 0.0005A^{1/3}E - 0.000001ZE^2]\sigma_R \ , \quad (3)$$

$$\sigma_{BF}^{p/n} = \sigma_{BU}^{p/n} - \sigma_{EB} \ , \quad (4)$$

leading to the total–breakup cross section:

$$\sigma_{BU} = \sigma_{EB} + 2\sigma_{BF}^{p/n} \ . \quad (5)$$

Equal BF cross sections for proton and neutron emission have been considered in the above expressions.

The latest BU parametrization, given by Kalbach [9] within the FENDL-3 project [10], considers also equal cross sections for the BU proton and neutron emission:

$$\sigma_{BU}^{p/n}(E) = 5.4(D_0)^2 exp(\frac{E}{170})[1 + exp(\frac{42 - E}{14})]^{-1} \ , \quad (6)$$

where

$$D_0 = 1.2\frac{5A^{\frac{1}{3}}}{1. + exp(\frac{E}{30})} + 1.2 \ .$$

As it can be seen in Figure 1, both Kalbach's parametrizations [8, 9] predict similar high values of total proton breakup cross sections at the lowest incident energies, even exceeding σ_R, while the latter predicts also lower values in comparison with the experimental systematics of the total proton–emission breakup fraction σ_{BU}^{p}/σ_R [12] (Figure 2). Regardless the differences between Kalbach [8] and Avrigeanu *et al.* [4] predictions at low deuteron energies, it results close values of the total proton–emission breakup cross sections within the energy range ∼10–60 MeV. From Figures 1 and 2 it can be observed that both parametrizations predict the increasing role of deuteron breakup with increasing the mass/charge of target nuclei. The very scarce experimental deuteron BU systematics [12] may lead to large uncertainties of the BU cross–section energy dependence at deuteron energies over 60 MeV. Therefore, only the extension of experimental data beyond this energy limit may improve the corresponding parametrizations.

Concerning the energy dependence of the inelastic- and elastic-breakup components, the interest of the deuteron activation cross sections for incident energies up to 60 MeV [1–3] has motivated an additional check [13] of the elastic-breakup parametrization extension beyond the energies formerly considered for the derivation of its actual form.

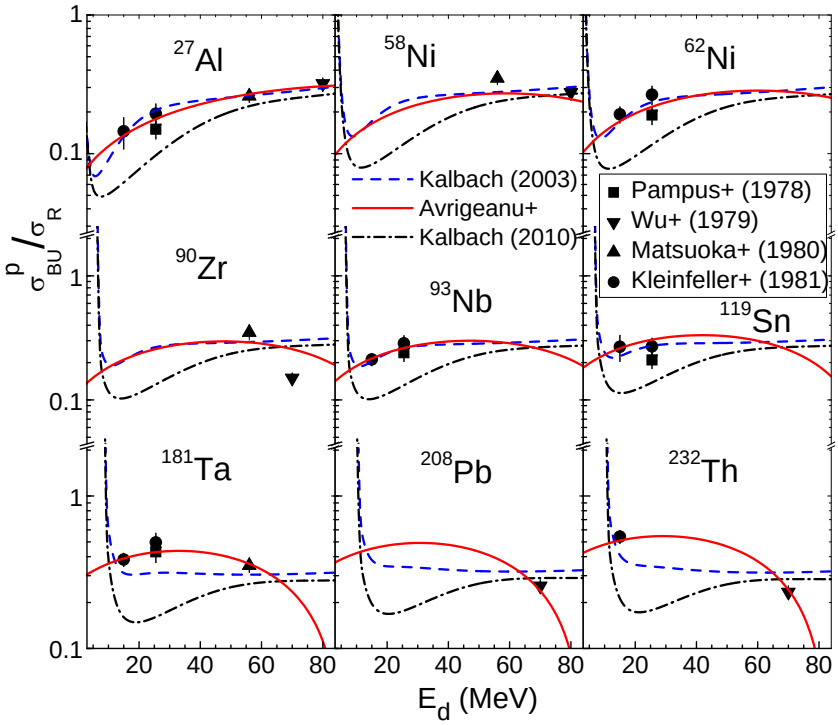

Figure 2. Comparison of experimental [12] total proton–emission breakup fraction and the corresponding parametrizations of Refs. [4] (solid curves), [8] (dashed curves), and [9] (dash–dotted curves), for deuteron interactions with target nuclei from ^{27}Al to ^{232}Th.

Actually, our parametrization [4] for the elastic-breakup was obtained from the analysis of the experimental systematics which covers an incident energy range from 15 to only 30 MeV. However, as it is shown in Figure 3(a,b) for (a) ^{63}Cu and (b) ^{93}Nb target nuclei, the elastic-breakup cross sections, σ_{EB}, (dashed curves), given by the empirical parametrization [4] decrease with the incident energy beyond the energy range within which it was established, while the total proton breakup cross sections, σ^{p}_{BU} (dotted curves) have an opposite trend. Therefore, in the absence of available experimental deuteron elastic-breakup data at incident energies above 30 MeV, the correctness of an eventual extrapolation should be checked by comparison of the related predictions with results of a theoretical model as, e.g., the Continuum-Discretized Coupled-Channels (CDCC) method [14–16].

The elastic-breakup component is treated within the CDCC formalism as an inelastic excitation of the projectile due to the nuclear and Coulomb interactions with the target nucleus by means of a three-body model, comprising the two-body projectile and the inert target. Consideration of this inelastic excitation is

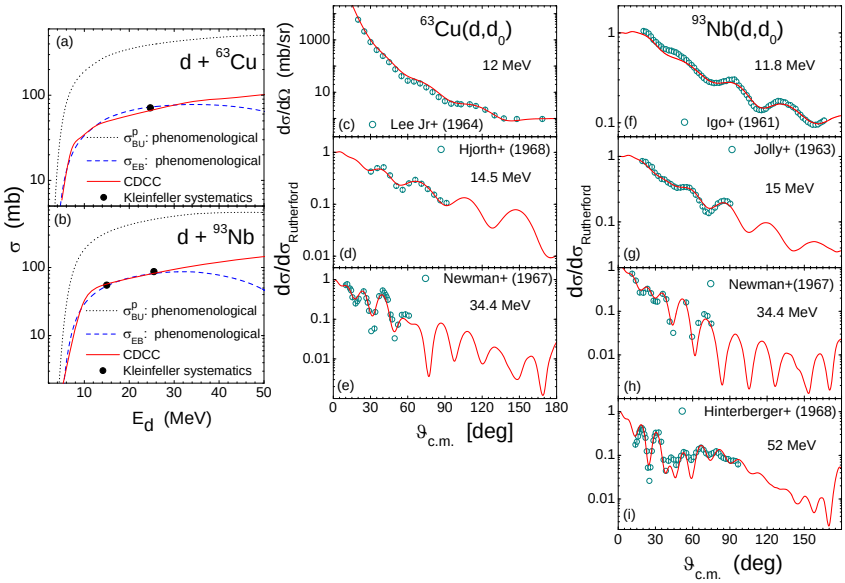

Figure 3. (a,b) Energy dependence of the empirical [4] (dashed curves) and CDCC [13] (solid curves) elastic breakup cross sections for deuteron scattering on ^{63}Cu and ^{93}Nb target nuclei. The solid circles are the values from Kleinfeller systematics [12]. By dotted curves are drawn the total proton breakup cross sections; (c-e) Comparison of measured and calculated (CDCC) angular distributions of deuteron elastic scattering on ^{63}Cu at E_d=12, 14.5, and 34.4 MeV, and (f-i) ^{93}Nb at E_d=11.8, 15, 34.4, and 52 MeV [18] (see text).

performed by coupling the projectile unbound excited states in the solution of the scattering problem through the coupled channels approach. Since the deuteron has no bound excited states, any excitation in the p-n coordinates will break up it into a proton and a neutron. In order to deal with a finite set of coupled equations, an essential feature of the CDCC method is the introduction of a discretization procedure, in which the continuum spectrum is represented by a finite and discrete set of square-integrable functions. The most widely used method of continuum discretization is the so-called *binning* method [14–16], in which the continuum spectrum is truncated at a maximum excitation energy ($E^*_{\rm max}$) and divided into a set of energy (or relative momentum) intervals. Each interval, or *bin*, is represented by a single square-integrable function, calculated by averaging the scattering states for the p-n relative motion within the bin width.

The energy dependence of the elastic-breakup cross sections provided by the excitation of the continuum spectrum (e.g., the population of the virtual excited states) in the case of the deuteron interaction with ^{63}Cu and ^{93}Nb target nuclei, is compared with the prediction of empirical parametrization [4] in Figure 3(a,b). The calculations were performed with the coupled-channels code

FRESCO [17]. The elastic-breakup cross sections corresponding to the Kleinfeller *et al.* systematics [12] are also shown. The agreement of the CDCC elastic-breakup cross sections [13] and the latter systematics can be considered as a validation of the present advanced model approach. Moreover, the comparison shown in Figure 3(a,b) points out that the CDCC calculations lead to elastic-breakup cross sections which follow the total-breakup cross section behavior, and makes clear that the empirical parametrization extrapolation for the elastic-breakup cross sections beyond the energies considered in this respect should be done with caution [13].

The check of the reliability of the CDCC parameters is given by the comparison between the experimental and the CDCC deuteron elastic-scattering angular distributions [13]. The good agreement of the experimental elastic-scattering angular distributions for deuteron interaction with ^{63}Cu and ^{93}Nb target nuclei [18] with the CDCC calculations shown in Figure 3(c-i) supports the consistent CDCC parametrization.

Overall, there are actually two opposite effects of the deuteron breakup on the deuteron activation cross sections that should be considered. Firstly, the total–reaction cross section, that is shared among different outgoing channels, is reduced by the value of the total breakup cross section σ_{BU}. On the other hand, the BF component, where one of the deuteron constituents interacts with the target nucleus, leading to a secondary composite nucleus, brings contributions to different reaction channels [4–7]. Thus, the absorbed proton or neutron following the deuteron breakup contributes to the enhancement of the corresponding (d, xn) or (d, xp) reaction cross sections, respectively.

In order to calculate the BF enhancement of, e.g., the (d, xn) reaction cross sections, the BF proton–emission cross section σ^{p}_{BF} should be multiplied by the ratios $\sigma_{(p,x)}/\sigma^{p}_{R}$, corresponding to the above–mentioned enhancing reaction, convoluted with the Gaussian line shape distribution of the breakup proton energy E_p for a given deuteron incident energy E. Finally, the integration over the breakup proton energy provides the BF enhancement cross section [5–7]:

$$\sigma^{p,x}_{BF}(E) = \sigma^{p}_{BF}(E) \int dE_p \frac{\sigma_{(p,x)}(E_p)}{\sigma^{p}_{R}} \frac{1}{(2\pi)^{\frac{1}{2}} w} \exp\Big[- \frac{(E_p - E^0_p(E))^2}{2w^2} \Big], \quad (7)$$

where σ^{p}_{R} is the proton total reaction cross section, x stands for various, e.g., γ, n, d, or α outgoing channels, while E^0_p and w are the centroid and standard deviation, respectively, of the above–mentioned breakup proton–energy Gaussian distribution given by Kalbach [8] related parameters. Interpolated values of the experimental nucleon–induced reaction cross sections from EXFOR library [18] have been involved within the BF enhancement estimation, e.g., Refs. [5–7], in order to reduce as much as possible the supplementary uncertainties brought by additional theoretical calculations.

The BF enhancements brought by BU protons and neutrons emitted during the deuteron interaction with ^{27}Al, ^{63}Cu, ^{65}Cu, ^{93}Nb, and ^{231}Pa through the

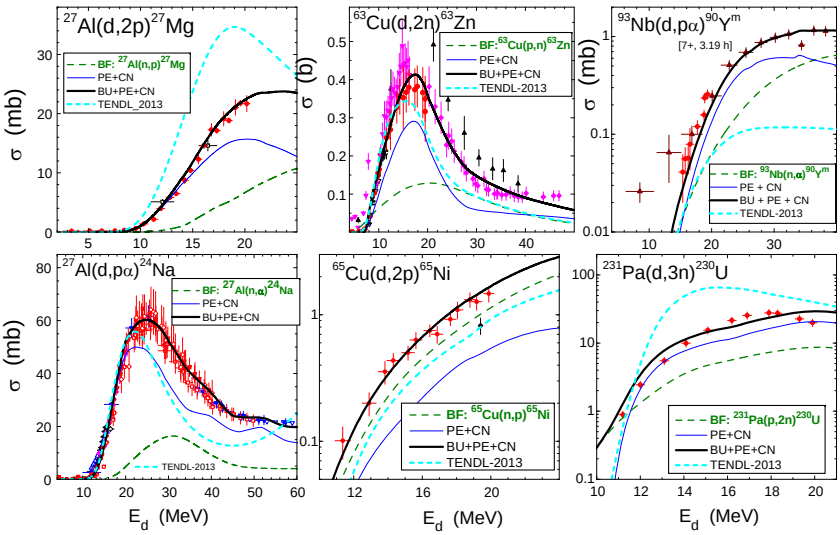

Figure 4. Comparison of measured deuteron activation cross sections [18], complete analysis results (thick solid curves) [5, 6] taking into account the BF enhancement (dashed curves) and PE+CN contributions (thin solid curves), and the TENDL-2013 [24] evaluations (dotted curves) (see text).

(n, p), (n, α), (p, n), and $(p, 2n)$ reactions populating various residual nuclei, are shown in Figure 4.

3 Transfer Reactions

Apart from the breakup contributions to deuteron interaction, an increased attention has to be devoted to the direct reactions (DR), very poorly accounted so far in deuteron activation analysis. The calculations of the DR mechanisms contributions, like stripping and pick–up, that are important at the low energy side of the (d, p), (d, n), (d, t), and (d, α) excitation functions [4–7], have been performed in the frame of the CRC formalism by using the code FRESCO [17].

The n–p effective interaction in the deuteron [19] as well as the d–n effective interaction in the triton [20] are assumed to have a Gaussian shape, while the Woods–Saxon shape [21] has been considered for the d–d effective interaction in the alpha particle. The transferred nucleon and deuteron bound states were generated in a Woods–Saxon real potential [4–7]. Concerning the (d, α) pick-up cross section calculation, the transfer of the deuteron cluster has been taken into account. The populated discrete levels and the corresponding spectroscopic factors for each DR type considered have been obtained from the ENSDF library [22] and Refs. therein. The importance of the stripping and pick–up reactions for the deuteron interaction process is evidenced in Figure 5.

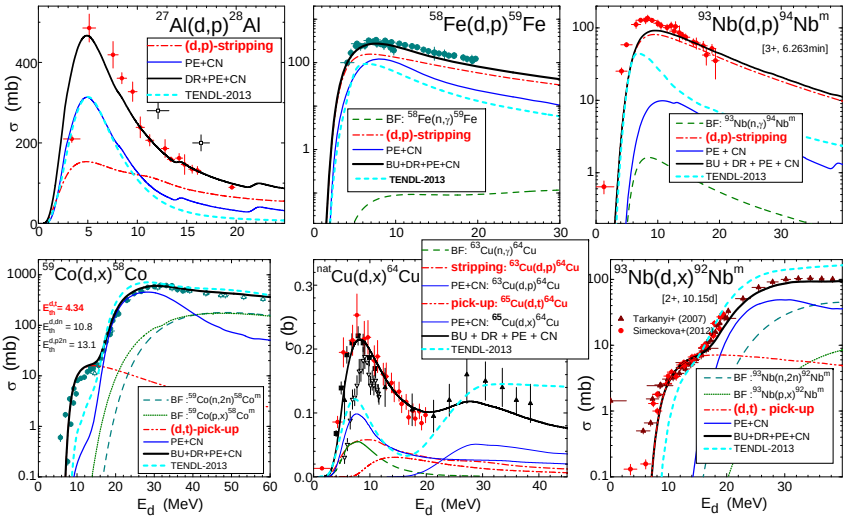

Figure 5. Comparison of measured deuteron activation cross sections ([18] and references therein), complete analysis results (thick solid curves) taking into account the BF enhancement (dashed curves), DR (dash–dotted and dash–dot–dotted curves) and PE+CN contributions (thin solid curves), and the TENDL-2013 [24] evaluations (dotted curves) (see text).

A particular note should concern the pick–up essential contribution to the total (d,t) activation cross section at the energies between its threshold and those for the (d,dn) and $(d,p2n)$ reactions that lead to the same residual nucleus. Thus, the pick–up component of the (d,t) excitation function is critical for the data description at deuteron incident energies lower than 10 MeV, where PE and CN contributions are almost negligible, see the bottom part of Figure 5.

4 Statistical Particle Emission

Following the decay path, the PE and CN reaction cross sections have been calculated by means of the code STAPRE-H [23], taking into account the deuteron total reaction cross section that remains available, through the correction for the incident flux leakage towards direct interactions (DI), i.e., the breakup, stripping and pick–up, as given by a reduction factor:

$$1 - \frac{\sigma_{BU} + \sigma_{(d,n)} + \sigma_{(d,p)} + \sigma_{(d,t)} + \sigma_{(d,\alpha)}}{\sigma_R} = 1 - \frac{\sigma^{DI}}{\sigma_R}. \qquad (8)$$

The energy dependence of this reduction factor (thick solid line), as well as of its components corresponding to deuteron interaction with the ^{56}Fe isotope is shown in Figure 6, pointing out the high contribution of the direct processes.

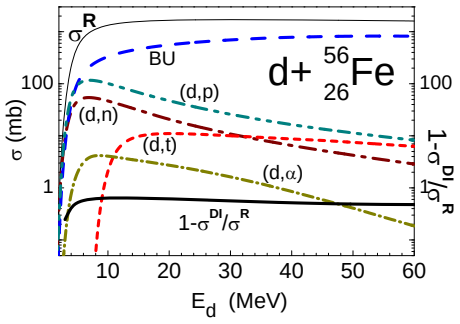

Figure 6. Total–reaction (thin solid curves), BU (dashed curves), stripping (d, n) (dash–dotted curves) and (d, p) (dash–dot–dotted curves), and pick–up (d, t) (dotted curves) and (d, α) (short dash–dotted curves) reaction cross sections for deuterons on ^{56}Fe, and the corresponding reduction factors of the deuteron flux going towards statistical processes (thick solid curves).

The local consistent parameters involved in the statistical calculations have been obtained or checked through the analysis of various independent experimental data, in advance to their use to obtain the deuteron–activation cross sections [5, 7]. Finally, the comparison between the experimental [18], calculated [5–7], and evaluated [24] deuteron activation cross sections are presented in Figures 4, 5. For each calculated activation cross section the reaction mechanisms contributions are shown. The mark BU, rather than BF, for the sum of various contributions to an activation cross section in Figures 4, 5 underlines the consideration of both breakup effects, i.e., the overall decrease of σ_R, as well as the BF enhancement. On the other hand, the apparent discrepancies between the experimental data and the corresponding evaluation stress out the effects of disregarding the direct processes within TENDL-2013 [24].

5 Conclusions

The overall agreement between the measured data and model calculations supports the description of nuclear mechanisms taken into account for the deuteron-nucleus interaction. However, while the associated theoretical frames are already settled for DR, PE and CN mechanisms, an increased attention should be given to microscopical description of the BF component. The improvement of deuteron breakup description requires complementary experimental studies involving deuterons, protons and neutron induced reactions too.

Acknowledgments

This work was partly supported by the Specific Grant Agreement F4E-GRT-168.02 of Fusion for Energy (F4E), and by a grant of the Romanian National

Authority for Scientific Research, CNCS - UEFISCDI, project number PN-II-ID-PCE-2011-3-0450.

References

[1] International Thermonuclear Experimental Reactor, http://www.iter.org/proj

[2] International Fusion Material Irradiation Facility (IFMIF), http://www.ifmif.org/b/

[3] Neutron For Science (NFS) project, Systéme de Production d'Ions Radioactifs en Ligne – generation 2, http://pro.ganil-spiral2.eu/spiral2/instrumentation/nfs

[4] M. Avrigeanu *et al.*, *Fusion Eng. Design* **84** (2009) 418-422.

[5] P. Bém *et al.*, *Phys. Rev. C* **79** (2009) 044610; E. Šimečková *et al.*, *Phys. Rev. C* **84** (2011) 014605; M. Avrigeanu *et al.*, *Nucl. Phys. A* **759** (2005) 327-341; *Phys. Rev. C* **88** (2013) 014612; *Phys. Rev. C* **89** (2014) 044613; *Nuclear Data Sheets* **118** (2014) 301-304.

[6] M. Avrigeanu, V. Avrigeanu, and A.J. Koning, *Phys. Rev. C* **85** (2012) 034603.

[7] M. Avrigeanu and V. Avrigeanu, *EPJ Web of Conferences* **2** (2010) 01004; *J. Phys: Conf. Ser.* **205** (2010) 012014; *J. Korean Phys. Soc.* **59** (2011) 903; *EPJ Web of Conferences* **21** (2012) 07003; *J. Phys: Conf. Ser.* **533** 012004 (2014).

[8] C. Kalbach Walker, "*Deuteron Breakup and 21Na Production*", Triangle University Nuclear Laboratory Progress Report **XLII** (2002-2003), p. 82-83; www.tunl.duke.edu/publications/tunlprogress/2003/.

[9] C. Kalbach Walker, "*Complete Phenomenological Model for Projectile-Breakup Reactions*", Report to the 2nd Research Co-ordination Meeting of the Fusion Evaluated Nuclear Data Library (FENDL) 3.0, 23-26 March 2010, IAEA, Vienna, and Refs. therein; http://www-nds.iaea.org/fendl3/vardocs.html.

[10] Fusion Evaluated Nuclear Data Library (FENDL), http://www-nds.iaea.org/fendl3/

[11] W.W. Daehnick, J.D. Childs, and Z. Vrcelj, *Phys. Rev. C* **21** (1980) 2253-2274.

[12] J. Pampus *et al.*, *Nucl. Phys. A* **311** (1978) 141-160; J.R. Wu, C.C. Chang, and H.D. Holmgren, *Phys. Rev. C* **19** (1979) 370-390; N. Matsuoka *et al.*, *Nucl. Phys. A* **345** (1980) 1-12; J. Kleinfeller *et al.*, *Nucl. Phys. A* **370** (1981) 205-230; M.G. Mustafa, T. Tamura, and T. Udagawa, *Phys. Rev. C* **35** (1987) 2077-2085.

[13] M. Avrigeanu and A.M. Moro, *Phys. Rev. C* **82** (2010) 037601.

[14] M. Kamimura *et al.*, *Prog. Theor. Phys. Suppl.* **89** (1986) 1-10, and Refs. therein.

[15] N. Austern *et al.*, *Phys. Rep.* **154** (1987) 125-204.

[16] A.M. Moro and F.M. Nunes, *Nucl. Phys. A* **767** (2006) 138-154.

[17] I.J. Thompson, *Comput. Phys. Rep.* **7** (1988) 167; v. FRES 2.3 (2007).

[18] Experimental Nuclear Reaction Data, http://www-nds.iaea.org/exfor/exfor.htm

[19] M. Kawai, M. Kamimura, and K. Takesako, *Prog. Theor. Phys. Suppl.* **89** (1986) 118-135.

[20] P. Guazzoni *et al.*, *Phys. Rev. C* **83** (2011) 044614.

[21] R.M. DelVecchio, *Phys. Rev. C* **7** (1973) 677-690.

[22] Evaluated Nuclear Structure Data File (ENSDF), http://www.nndc.bnl.gov/ensdf/

[23] M. Avrigeanu and V. Avrigeanu, IPNE Report NP-86-1995, Bucharest, 1995, and Refs. therein; *News NEA Data Bank* **17** (1995) 22.

[24] A.J. Koning and D. Rochman, *TENDL-2013: TALYS–Based Evaluated Nuclear Data Library*, 2013, http://www.talys.eu/tendl-2013/